RESEARCH ARTICLE

Macromolecular Chemistry and Physics
www.mcp-journal.de

Thermal Stable and Flexible Bio-Based Polybenzoxazine with Epoxy-Functionalized Poly(dimethylsiloxane) Hybrids

*Yang-Chin Kao, Wei-Cheng Chen, Ahmed F. M. EL-Mahdy, Mohamed Gamal Mohamed, Mohsin Ejaz, and Shiao-Wei Kuo**

In this study, a monofunctionalized bio-based benzoxazine monomer (VAnBZ-CN) is synthesized by condensation of vanillin, formaldehyde, and aniline, and a bifunctional epoxy-functionalized poly(dimethylsiloxane) (PDMS-epoxy) is also prepared through hydrosilylation reactions with allyl glycidyl ether. By blending the inorganic PDMS-epoxy with the VAnBZ-CN benzoxazine monomer, an organic/inorganic hybrid material is formed, which exhibited enhanced thermal stability after thermal curing polymerization. The improved thermal stability observed in the hybrid material can be attributed to a combination of the formation of the triazine structure by VAnBZ-CN and the presence of the inorganic part of PDMS-epoxy on the surface. For example, the PDMS-epoxy/VAnBZ-CN = 1/1 hybrid showed the thermal decomposition temperature (T_{d10}) of 309 °C, the glass transition temperature (T_g) of 165 °C, and the char yield of 54 wt.% after the thermal curing polymerization process conducted at 240 °C based on thermogravimetric (TGA) and dynamic mechanical analyses (DMA). Furthermore, the char yield of the hybrid material with PDMS-epoxy/VAnBZ-CN = 1/3 is higher than that both of pure VAnBZ-CN and PDMS-epoxy after the thermal curing polymerization process. This result indicates that the addition of PDMS-epoxy resin can improve the formation of a char residue and then enhance the resistance to thermal decomposition for their overall thermal stabilities.

1. Introduction

In recent years, there has been significant research on benzoxazines (BZ) as the thermosetting resins ascribable to their exceptional properties such as good electrical resistance, flexible molecular design, excellent flame retardancy, high thermal and dimensional stability, and low surface free energy.[1–14] Derivatives of BZ, comprising six-membered heterocyclic rings, could be synthesized through the Mannich condensation process involving phenols, formaldehyde, and primary aromatic or aliphatic amines.[15–17]

Epoxy resins are also widely reckoned as thermosetting polymers with excellent performance characteristics, making them suitable for a range of applications such as adhesives, automotive components, coatings, composites, semiconductor encapsulation, and paint. Particularly, epoxy resins that incorporate aromatic units have gained considerable attention.[18–23] Epoxy resin is comprised of two or more reactive epoxide functional groups, which can undergo polymerization with hardeners such as amines, phenols, carboxylic acids, thiols, catalysts, or anhydrides to form organic resin polymers.[24–28] However, conventional epoxy resins are unable to meet the requirements for thermal or flame resistance. In order to address this limitation, high thermal stability polymers such as benzoxazine,[23,29] bismaleimides,[30,31] cyanate esters,[32,33] and polyethersulfone[34] are often incorporated into epoxy resins to escalate their properties.

Poly(dimethylsiloxane) (PDMS) has many unique characteristics, for example, low glass transition temperatures (T_g), low surface free energy, high moisture resistance, low-stress resistance, thermo-oxidative stability, and flexibility. The incompatibility of epoxy and PDMS at thermodynamic stability imposes limitations on their ability to form a homogeneous mixture, which usually exhibits two separate T_g values.[35–40] Therefore, PDMS modified by reactive end groups such as amino, epoxy, or vinyl groups have been incorporated into the epoxy system to overcome this problem.[41]

In this study, we have developed organic/inorganic hybrid materials by combining benzoxazine, epoxy, and PDMS units. The synthesis involved the condensation of a mono-functionalized bio-derived benzoxazine monomer (VAnBZ-CN) derived from

Y.-C. Kao, W.-C. Chen, A. F. M. EL-Mahdy, M. G. Mohamed, M. Ejaz, S.-W. Kuo
Department of Materials and Optoelectronic Science
Center for Functional Polymers and Supramolecular Materials
National Sun Yat-Sen University
Kaohsiung 804, Taiwan
E-mail: kuosw@faculty.nsysu.edu.tw
M. G. Mohamed
Chemistry Department
Faculty of Science
Assiut University
Assiut 71516, Egypt
S.-W. Kuo
Department of Medicinal and Applied Chemistry
Kaohsiung Medical University
Kaohsiung 807, Taiwan

The ORCID identification number(s) for the author(s) of this article can be found under https://doi.org/10.1002/macp.202300153

DOI: 10.1002/macp.202300153

a vanillin derivative (V-CN),[7] formaldehyde (CH_2O), and aniline, along with a bifunctional epoxy-propyl polydimethylsiloxane (PDMS-epoxy) synthesized through the hydrosilylation of PDMS and allyl glycidyl ether. This synthetic approach offers several advantages. Firstly, it eliminates the use of epichlorohydrin, which can be harmful to human health, and instead incorporates PDMS and naturally sourced vanillin, making it a more environmentally preferable choice. Notably, the chlorine-free nature of the PDMS synthesis method is particularly advantageous. The resulting hybrid material exhibits improved thermal stability, which could be attributed to two factors. Firstly, the formation of the triazine structure by VAnBZ-CN contributes to the improvement of thermal stability. Secondly, the presence of the inorganic part of PDMS-epoxy on the material's surface aids in the formation of a char residue. The char residue improves the material's resistance to decomposition and overall thermal stability. Thus, the addition of PDMS-epoxy not only enhances the compatibility of the components but also improves the thermal properties and resistance to the decomposition of the hybrid material.

2. Experimental Section

2.1. Materials

Poly(dimethylsiloxane) (PDMS) with a molecular weight (M_n) of 580 g mol^{-1}, toluene, 1,4-dioxane, aniline, and *p*-phenylenediamine (PDA) were procured from Sigma–Aldrich. Allyl glycidyl ether was obtained from Thermo Fisher Scientific. The synthesis of 2-(4-hydroxy-3-methoxybenzylidene)malononitrile (V-CN) was conducted following the previously reported method.[7]

2.2. Synthesis of Bis-epoxypropoxy poly(dimethylsiloxane) (PDMS-epoxy)

PDMS (20.00 g, 34.4 mmol) and allyl glycidyl ether (8.66 g, 75.8 mmol) were combined, and toluene (200 mL) was added to the flask equipped with the reflux condenser. Pt(dvs) (3 drops) was then added dropwise to the mixture, which was subsequently heated at 75 °C for 48 h under a nitrogen (N_2) atmosphere. Afterward, the mixture underwent charcoal filtration, and the filtrate was concentrated using vacuum distillation. The concentrated filtrate was dried in a vacuum oven at 75 °C, resulting in the formation of a transparent liquid (24.32 g, 87% yield).

2.3. Synthesis of 2-((8-methoxy-3-phenyl-3,4-dihydro-2H-benzo[e][1,3]oxazin-6-yl)methylene) Malononitrile (VAnBZ-CN)

In this experiment, 2-(4-hydroxy-3-methoxybenzylidene)malononitrile (V-CN) (0.50 g, 2.5 mmol), formaldehyde (CH_2O) (0.18 g, 6.2 mmol), and 1,4-dioxane (30 mL) were mixed in the flask equipped with the reflux condenser. The mixture was placed under a nitrogen (N_2) atmosphere, and aniline (0.23 g, 2.5 mmol) was added. A reaction mixture was then heated at 110 °C for 24 h. After completion, a mixture was filtered, and the solvent was removed by using the rotary evaporator. The resulting residue was further dried in the vacuum oven and to purify the product, the residue was subjected to column chromatography by using silica gel (SiO_2) as the stationary phase and a hexane/ethyl acetate (EtOAc) mixture (1:1) as the mobile phase. This purification step yielded a yellow powder identified as VAnBZ-CN (0.24 g, 30% yield).

2.4. Preparation of PDMS-epoxy/PDA and PDMS-epoxy/VANBZ-CN Hybrids

The casting samples were carefully placed into the aluminum tray. Different molar ratios of PDMS-epoxy and *p*-phenylenediamine or VAnBZ-CN hybrids were mixed together for 48 h at 110 °C under vacuum conditions. Subsequently, the mixture underwent thermal polymerization for 2 h at temperatures of 150, 180, 210, and 240 °C, respectively. As a result, the final PDMS-epoxy hybrids with a dark color were obtained.

3. Results

3.1. The Preparation of PDMS-Epoxy Resin

In **Figure 1**a, the synthesis of the PDMS-epoxy compound from PDMS is shown, involving a hydrosilylation reaction. The success of this reaction was confirmed through the analysis of FTIR, ^{1}H NMR, and TGA as depicted in Figure 1b–d. In Figure 1b, a comparison of the FTIR spectra of PDMS and PDMS-epoxy compounds is presented. The PDMS derivatives exhibited a weak signal at 1261 cm^{-1}, corresponding to the Si–CH_3 unit, and strong signals at 1030 and 1092 cm^{-1}, indicating the presence of the Si–O–Si unit. Additionally, a weak signal at 910 cm^{-1}, associated with the epoxide functional group, was observed in the PDMS-epoxy compound. The absence of the Si–H unit at 2130 cm^{-1} indicated the successful completion of the hydrosilylation reaction. Figure 1c displays comparable ^{1}H NMR spectra of PDMS and PDMS-epoxy compounds. The Si–CH_3 protons, initially observed at 0.07 to 0.19 ppm in PDMS, were shifted to 0.04 to 0.08 ppm after the hydrosilylation reaction, indicating increased shielding due to the Si–CH_2 unit acting as a donating group. The presence of the epoxide functional group in PDMS-epoxy was indicated by peaks *h*, *i*, and *g* at 2.61 ppm (trans protons), 2.80 ppm (trans protons), and 3.15 ppm (protons), respectively. Various signals for aliphatic protons were observed between 0.52 and 3.71 ppm. Figure 1d demonstrates the corresponding TGA thermograms of PDMS and PDMS-epoxy compounds. The thermal degradation temperature was observed to increase after the hydrosilylation reaction, suggesting an improvement in thermal stability.

3.2. Synthesis of VAnBZ-CN Monomer

In Figure S1 (Supporting Information), we presented our synthetic method for VAnBZ-CN through Mannich condensation. We utilized V-CN, characterized by broad absorption bands at 3417 cm^{-1} for the phenolic OH group and the sharp peak at 2227 cm^{-1} for the CN unit, to react with CH_2O and aniline at

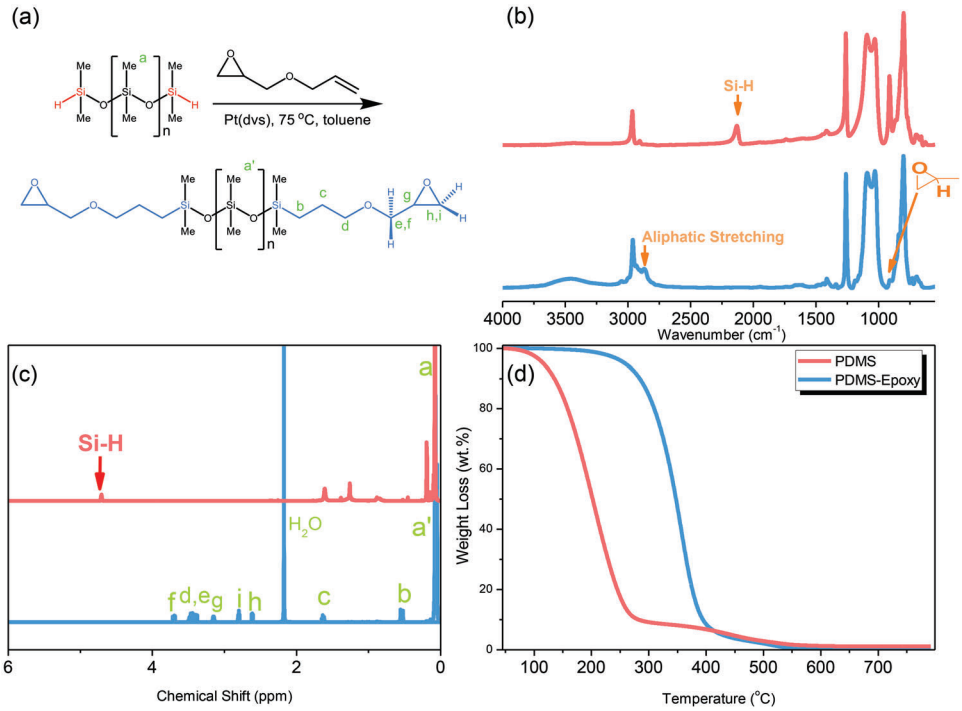

Figure 1. a) The synthesis of PDMS-epoxy and the corresponding b) FTIR, c) ^{1}H NMR spectra, and d) TGA analyses of PDMS and PDMS-epoxy resin.

110 °C in 1,4-dioxane. After the Mannich condensation reaction, VAnBZ-CN no longer exhibited an absorption band for the O-H bond and instead showed the new absorption peak at 934 cm^{-1} due to the BZ ring units. Additionally, the presence of an oxazine ring in VAnBZ-CN was confirmed through the observation of two signals at 4.72 ppm (*b*) and 5.63 ppm (*a*), corresponding to the $ArCH_2N$ and OCH_2N groups, respectively, as shown in **Figure 2**d. Furthermore, VAnBZ-CN displayed signals at 8.28 ppm, 6.46 to 7.50 ppm, and 3.75 ppm, representing the protons of conjugated C=C–H, aromatic C–H, and O–CH_3 units, respectively.

Figure 2a displays the DSC analyses performed on VAnBZ-CN before and after undergoing a thermal curing polymerization with a heating rate of 20 °C min^{-1}. The uncured VAnBZ-CN monomer exhibited a melting point of 150 °C and an exothermic curing peak at 243 °C. After thermal curing polymerization at 150 °C, the melting point of VAnBZ-CN was decreased to 147 °C, and the exothermic curing peak was still observed at 243 °C. Additionally, as the thermal curing temperature increased from 180 to 210 °C, the exothermic curing temperature shifted to higher values, and the melting point disappeared. At 240 °C, the exothermic curing peak disappeared, and pyrolysis was observed, as shown in Figure 2c. The effect of thermal curing on VAnBZ-CN monomer was further examined through FTIR spectra. Pure VAnBZ-CN exhibited signals for the CN unit at 2224 cm^{-1} and the BZ ring unit at 934 cm^{-1} in Figure 2b. After thermal curing polymerization, the intensities of the CN units and BZ ring units were decreased, while new absorption peaks at 1377 and 1615 cm^{-1} appeared, which suggested CN units underwent a gradual transformation into triazine structures. In the TGA analyses, the uncured VAnBZ-CN monomer showed a distinct thermal decomposition temperature of 192 °C and a char yield of 34 wt.% in Figure 2c. After undergoing thermal polymerization, the T_{d10} values were observed to be 181, 264, 304, and 369 °C, respectively, and the corresponding char yields were 23, 38, 52, and 59 wt.% as displayed in Figure 2c. With an increase in the thermal treatment temperature, VAnBZ-CN formed the cross-linked network structure with the aromatic triazine ring by the thermal reaction of CN groups. Additionally, thermal cracking occurred at high temperatures, resulting in excellent thermal stability as confirmed by FTIR spectra and TGA thermograms.

3.3. The Preparation of PDMS-Epoxy/PDA and PDMS-Epoxy/VAnBZ-CN

In **Figure 3**a, FTIR spectra of PDMS-epoxy/PDA and PDMS-epoxy/VAnBZ-CN hybrids are presented. As the ratio of VAnBZ-CN increased in the hybrids, it was observed that the intensity of CN unit (at 2224 cm^{-1}) and BZ ring units (at 934 cm^{-1}) also increased, while the intensity of Si–O–Si bonds (at 1030 and 1092 cm^{-1}) decreased. Additionally, these hybrids exhibited broad absorption bands ranging from 3000 to 3615 cm^{-1}, suggesting the ring-opening of the epoxide group and BZ ring. Figure 3b,c displays the DSC and TGA analyses of PDMS-epoxy hybrids, pure PDMS-epoxy, and pure VAnBZ-CN using the heating rate of 20 °C/min. As the amount of PDMS-epoxy increased into the VAnBZ-CN monomer, the exothermic curing temperature of the hybrids shifted to a lower temperature range, from 266 to 203 °C. Additionally, the char yield of the hybrids decreased, suggesting that the incorporation of VAnBZ-CN allowed for the formation of triazine structures that enhanced thermal stability. Figure 3d illustrates the possible mechanism for the thermal curing polymerization of PDMS-epoxy/VAnBZ-CN hybrids.[42]

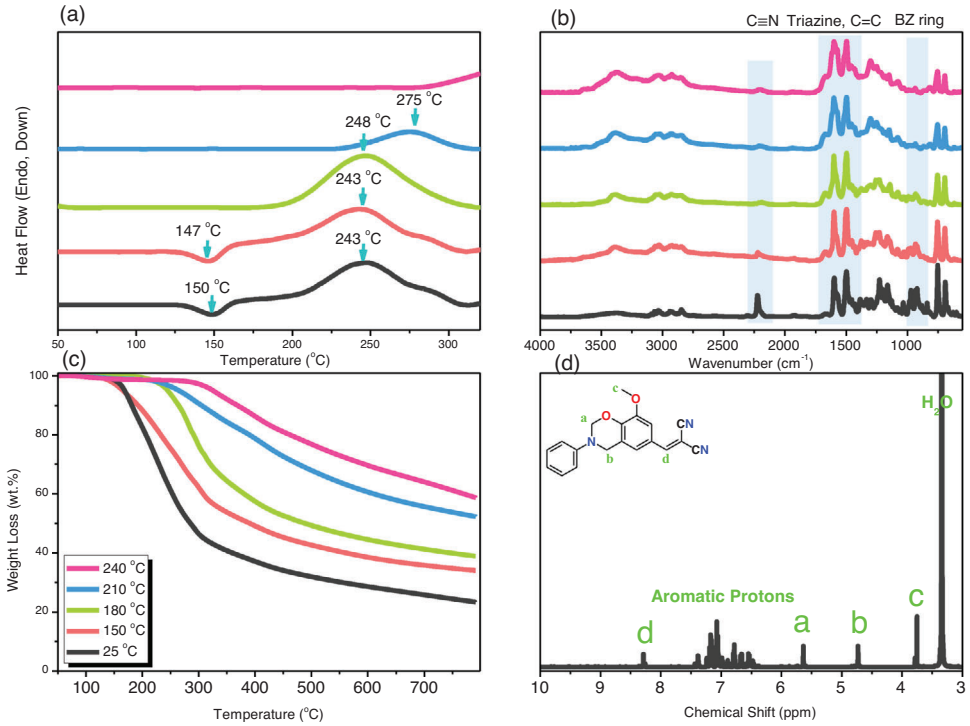

Figure 2. a) Dynamic DSC thermal analyses, b) FTIR spectra, c) TGA analyses, and d) ^{1}H NMR spectra of VAnBZ-CN monomer.

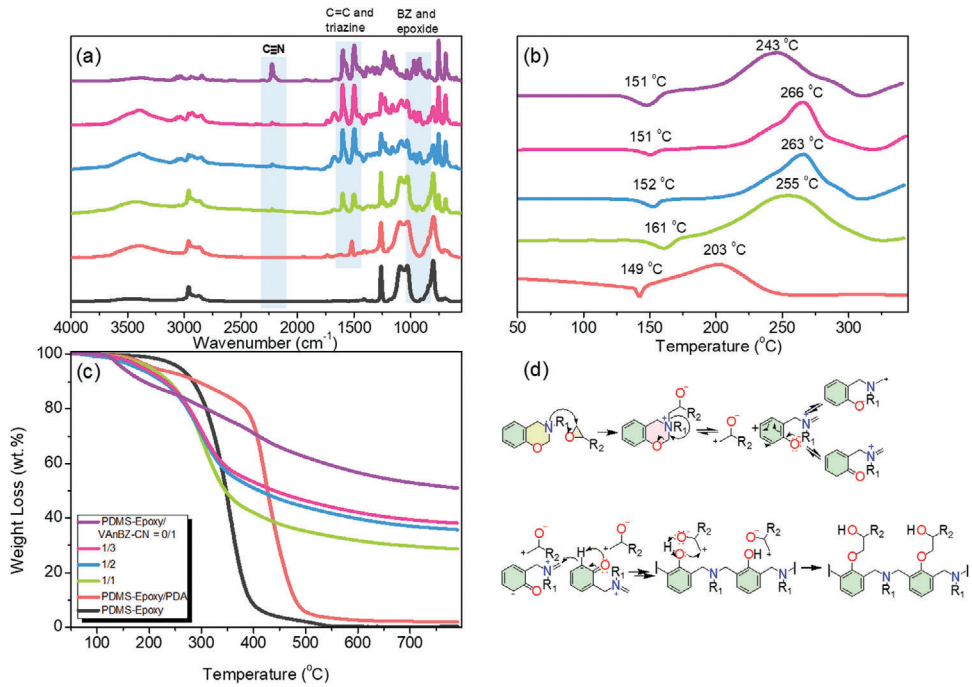

Figure 3. a) FTIR, b) DSC, c) TGA analyses of PDMS-epoxy, VAnBZ-CN, and their hybrids, and d) ring-opening reaction of epoxy with benzoxazine to form cross-linked network structures.

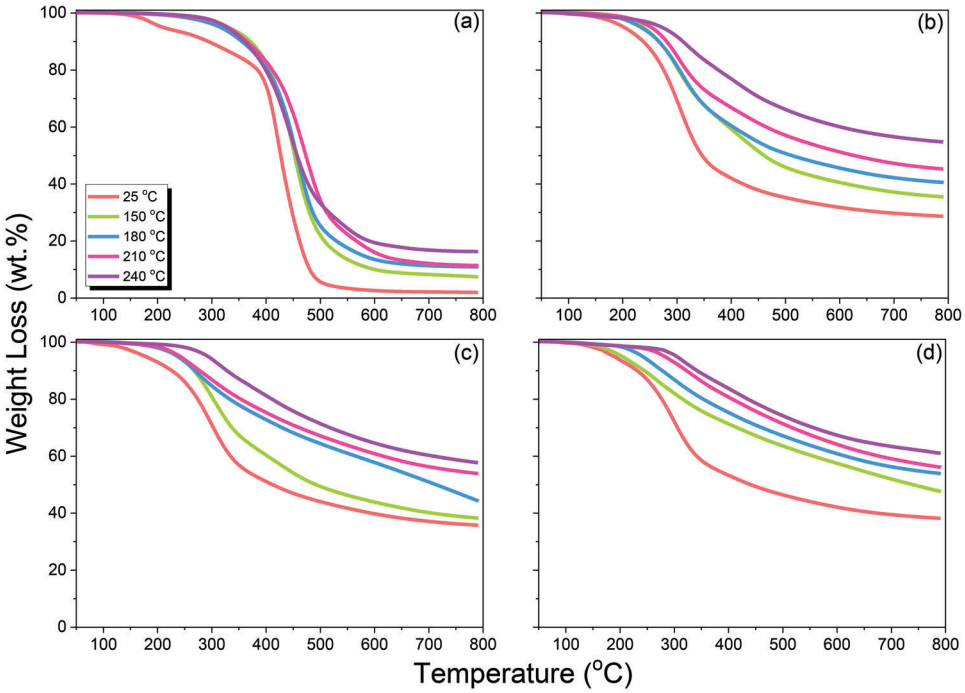

Figure 4. TGA analyses of pure PDMS-epoxy resin and its hybrids of a) PDMS-epoxy/PDA = 1/1 hybrid and various PDMS-epoxy/VAnBZ-CN of b) 1/1, c) 1/2, and d) 1/3 hybrids during thermal curing polymerization at each temperature.

3.4. Thermal and Mechanical Properties of PDMS-Epoxy Hybrids

Figure 4 illustrates the TGA analyses conducted on various PDMS-epoxy hybrids to examine the impact of different thermal-polymerization temperatures. The findings reveal that the thermal resistance of the PDMS-epoxy matrix improved following thermal polymerization, as indicated by increased T_{d10} (temperature at 10% weight loss) and char yield values. These results suggest the formation of crosslinking structures between PDA and VAnBZ-CN in the epoxy matrix. At elevated temperatures, the inorganic component of PDMS gradually migrates to the surface of the hybrids, resulting in the formation of a dense silica layer, which acts as the barrier, impeding the penetration of oxygen into the deeper regions of the mixture. Comparatively, the PDMS-epoxy/PDA hybrids exhibit higher T_{d10} values and lower char yield values in comparison to the PDMS-epoxy/VAnBZ-CN hybrids. **Figure 5**c,d provides a summary of the T_{d10} and char yield values, respectively, for all the hybrid samples. Figure 5c,d shows that the char yield of PDMS-epoxy hybrids increases with the concentration of VAnBZ-CN. This observation is in line with expectations, as the triazine structure formed by VAnBZ-CN is anticipated to enhance thermal stability. However, interestingly, the T_{d10} value of PDMS-epoxy/PDA hybrids was higher (360 °C) compared to PDMS-epoxy/VAnBZ-CN hybrids (309 °C) after thermal curing polymerization at 240 °C due to the low content of inorganic PDMS in the PDMS-epoxy/VAnBZ-CN hybrids.

Despite the lower T_{d10} value, a char yield value of PDMS-epoxy/VAnBZ-CN = 1/1 hybrid was significantly higher at 54 wt.% compared to PDMS-epoxy/PDA hybrids, which yielded only 16 wt.% after the same thermal curing polymerization at 240 °C. This suggests that the formation of a silica layer could enhance the thermal resistance of the hybrids. Notably, even the char yield of PDMS-epoxy/VAnBZ-CN = 1/3 hybrid was higher than that of pure VAnBZ-CN after the thermal curing polymerization process at 240 °C, further supporting the role of the silica layer in improving thermal resistance.

Figure 5a presents the DSC thermograms of PDMS-epoxy/PDA = 1/1 hybrid before and after each thermal curing polymerization process. The thermograms revealed an enthalpy of fusion at 149 °C, corresponding to the melting point of PDA. Furthermore, an exothermic peak observed at 203 °C indicated that the amino-functional group-initiated ring-opening and self-polymerization reactions in the epoxide group, as depicted in Figure 5b.[25] Following the thermal-polymerization process, both the melting point and the exothermic peak disappeared, suggesting the completion of the polymerization reactions.

Figure 6a displayed the DSC analyses of PDMS-epoxy/VAnBZ-CN = 1/1 hybrid before and after each thermal curing polymerization process. The analyses showed a melting point at 161 °C before and after undergoing thermal polymerization at 150 °C. With increasing in the thermal treatment temperature, the melting point vanished. Furthermore, the exothermic curing peaks shifted to lower values from 25 to 180 °C. After thermal polymerization at 210 °C, the exothermic curing peak observed at 277 °C signified alkene group could carry out polymerization. At 240 °C, the exothermic curing peak vanished, and pyrolysis was observed, as exhibited in Figure 4b. Figure 6b displays the FTIR analyses of these hybrids, gauged before and after thermal polymerization at 150, 180, 210, and 240 °C. The FTIR spectrum of the PDMS epoxy resin revealed an absorption peak at 910 cm^{-1} and that of VAnBZ-CN exhibited signals for BZ ring at 934 cm^{-1} and the CN units at 2223 cm^{-1} [7] After thermal

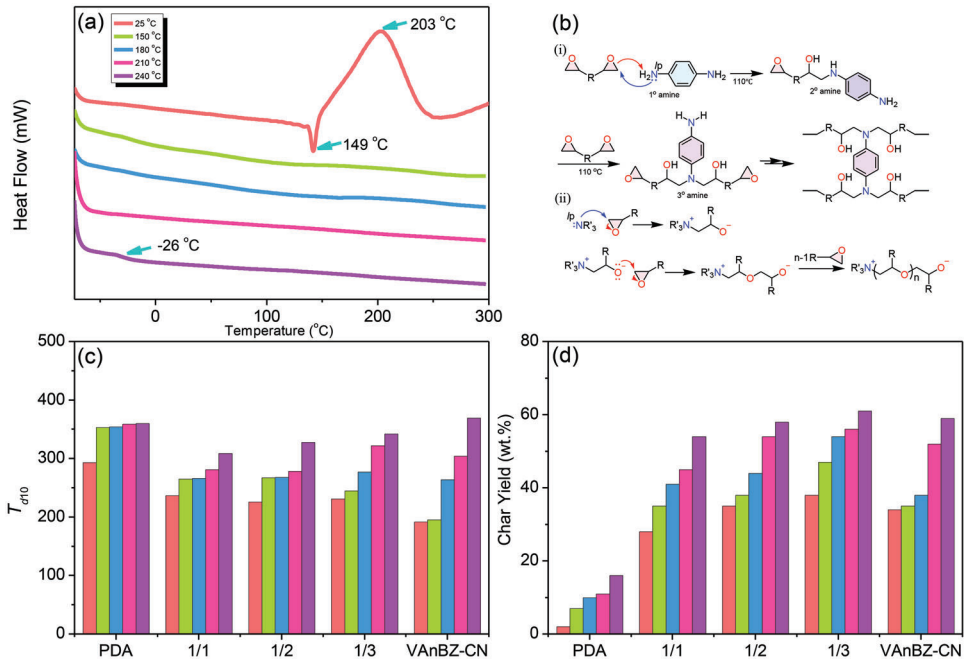

Figure 5. a) DSC analyses of PDMS-epoxy/PDA hybrid, b) ring-opening reactions of epoxy, and the corresponding c) T_{d10} values and d) char yields of PDMS-epoxy/PDA hybrid after thermal curing polymerization procedures.

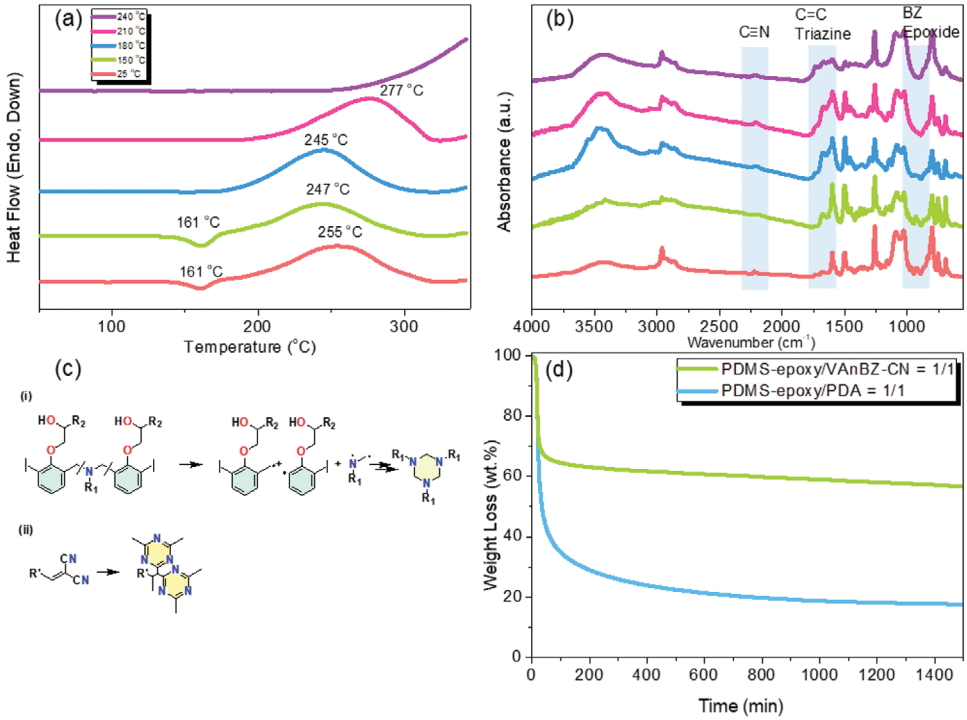

Figure 6. a) DSC analyses and b) FTIR spectra of PDMS-epoxy/VAnBZ-CN = 1/1 hybrid, c) the mechanism of the formation of the triazine ring of VAnBZ-CN at high temperature, and d) TGA profiles of PDMS-epoxy/PDA = 1/1 and PDMS-epoxy/VAnBZ-CN = 1/1 hybrids after thermal curing polymerization at 240 °C and then remained at 400 °C for 24 h.

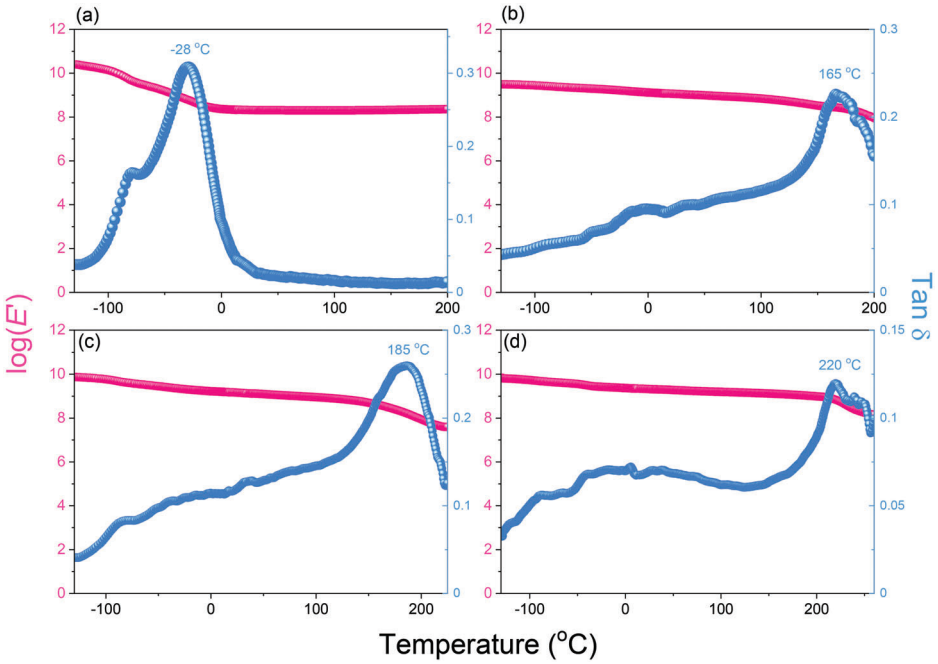

Figure 7. DMA analyses of a) PDMS-epoxy/PDA = 1/1 hybrid and the various PDMS-epoxy/VAnBZ-CN hybrids of b) 1/1, c) 1/2, and d) 1/3 after thermal curing polymerization at 240 °C.

polymerization at each temperature, both units of signals decreased and eliminated. Moreover, a significant and broad signal for hydroxyl group stretching showed up at 3000 to 3615 cm^{-1}, pointing out that the ring-opening of PDMS epoxy and BZ ring had occurred, with the increase of the signals for triazine units appearing at 1363 and 1635 cm^{-1}. In addition, the signal for the Si–O–Si units of these hybrids became broad after thermal polymerization, recommending that the OH group of PDMS epoxy and VAnBZ-CN formed hydrogen bonds with the Si–O–Si units of PDMS.[43–44] Figure 6c displays the mechanism of generation of triazine rings through the thermal reaction of cyano groups and thermal cracking produces at high temperatures.[45–47] Figure 6d displays TGA analyses comparing PDMS-epoxy/PDA and PDMS-epoxy/VAnBZ-CN hybrids after thermal curing polymerization at 240 °C, followed by exposure to 400 °C for various durations. The results clearly demonstrated that the incorporation of VAnBZ-CN monomer in the PDMS-epoxy resin significantly enhanced the thermal stability of these hybrids. For instance, a char yield value of PDMS-epoxy/VAnBZ-CN = 1/3 hybrid reached an impressive 56 wt.% after 24 h at 400 °C, while the PDMS-epoxy/PDA hybrid only achieved 17 wt.%. This finding highlights the superior thermal resistance conferred by the presence of VAnBZ-CN, underscoring its effectiveness in enhancing the stability of the hybrid materials under high-temperature conditions.

Figure 7 depicts DMA thermal analyses conducted on PDMS-epoxy/PDA and various PDMS-epoxy/VAnBZ-CN hybrids following thermal curing polymerization at 240 °C. The measurements focused on the loss tan δ, which represents the T_g, and the storage modulus (E''), reflecting mechanical properties. For the PDMS-epoxy/VAnBZ-CN = 1/1 hybrid, the storage modulus at 25 °C was determined to be 1128 MPa, with a corresponding T_g value of 165 °C. In contrast, the PDMS-epoxy/PDA hybrids exhibited lower initial E'' and T_g values, specifically 208 MPa and −28 °C, respectively, as observed in Figure 7a, which is consistent with DSC analysis (T_g = −26 °C) in Figure 5a.

As the concentration of VAnBZ-CN increased in the PDMS-epoxy resin, both the E' and T_g values also increased. For instance, the PDMS-epoxy/VAnBZ-CN = 1/2 hybrid displayed E' and T_g values of 1446 MPa and 185 °C, respectively. Similarly, the PDMS-epoxy/VAnBZ-CN = 1/3 hybrid demonstrated E' and T_g values of 1448 MPa and 220 °C, respectively. These findings indicate that higher concentrations of VAnBZ-CN result in improved mechanical properties, reflected by increased storage modulus and elevated glass transition temperatures.

Figure 8 includes SEM images that provide crucial insights into the dispersion of inorganic PDMS-epoxy within the benzoxazine resin. Figure 8a,b displays SEM images at different magnifications of PDMS-epoxy/VAnBZ-CN = 1/1 hybrid after thermal curing polymerization at 240 °C. Both SEM images depict the featureless morphology without any observable macro-phase separation, implying the uniform dispersion of inorganic PDMS within the benzoxazine matrix. Furthermore, the Si-, C-, and O-mapping analysis confirms the even distribution of PDMS on the surface of the benzoxazine resin. The mapping results indicate that silicon (Si) is present throughout the surface, along with carbon (C) and oxygen (O), indicating the presence of PDMS. Additionally, the red points in Figure 8c, corresponding to the Si-mapping, highlight the PDMS-rich domains, which further support the well-dispersed nature of flexible PDMS within the benzoxazine matrix.

4. Conclusions

The PDMS-epoxy resin was prepared through a hydrosilylation reaction, utilizing the Si–H functional groups of PDMS. The

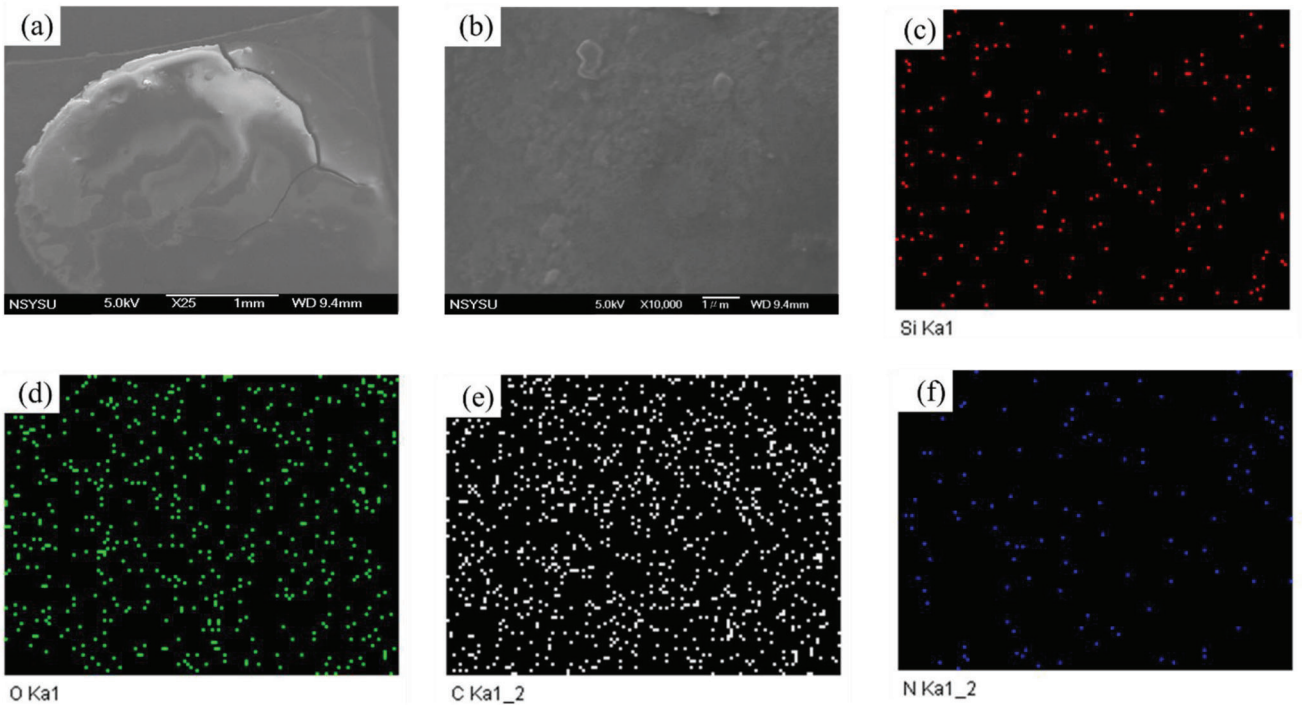

Figure 8. (a,b) SEM images of PDMS-epoxy/VAnBZ-CN = 1/1 hybrid and the corresponding c) Si, d) O, e) C, and f) N-mapping after thermal curing polymerization [Scale bar; 1 mm and 1 μm].

VAnBZ-CN monomer, derived from V-CN, aniline, and CH_2O, was used in the preparation. The incorporation of VAnBZ-CN in the hybrids resulted in higher char yield compared to the PDA hybrid during thermal curing polymerization. This can be attributed to the triazine structure of VAnBZ-CN, which promotes the formation of carbon residue. Moreover, after thermal curing polymerization at 240 °C, the char yield of VAnBZ-CN hybrids exceeded that of conventional PDA hybrids. This can be attributed to the development of a silica layer on the surface of the hybrid, which inhibits the contact of oxygen. DMA and TGA analyses indicated T_g and char yield values of 220 °C and 61 wt.%, respectively, for the PDMS-epoxy/VAnBZ-CN hybrids. These values were expressively higher than those achieved with the typical organic curing agents in the PDMS-epoxy matrix. SEM images further revealed the uniform dispersion of inorganic PDMS within the benzoxazine resin. This dispersion is facilitated by covalent bonding between the epoxy group and the benzoxazine ring, ensuring a homogeneous distribution of PDMS in the hybrid system.

Supporting Information

Supporting Information is available from the Wiley Online Library or from the author.

Acknowledgements

This study was supported financially by the Ministry of Science and Technology, Taiwan, under contracts NSTC 110-2124-M-002-013 and 111-2223-E-110-004.

Conflict of Interest

The authors declare no conflict of interest.

Data Availability Statement

Research data are not shared.

Keywords

benzoxazine resins, PDMS, ring-opening polymerizations, thermal stability

Received: May 23, 2023
Revised: June 10, 2023
Published online: July 2, 2023

[1] Y. Lyu, H. Ishida, *Prog. Polym. Sci.* **2019**, *99*, 101168.
[2] C. J. Higginson, K. G. Malollari, Y. Xu, A. V. Kelleghan, N. G. Ricapito, P. B. Messersmith, *Angew. Chem., Int. Ed.* **2019**, *131*, 12399.
[3] M. G. Mohamed, T.-C. Chen, S.-W. Kuo, *Macromolecules* **2021**, *54*, 5866.
[4] Y. Lu, J. Liu, W. Zhao, K. Zhang, *Chem. Eng. J.* **2023**, *457*, 141232.
[5] M. G. Mohamed, M. M. Samy, T. H. Mansoure, C.-J. Li, W.-C. Li, J.-H. Chen, K. Zhang, S.-W. Kuo, *Int. J. Mol. Sci.* **2022**, *23*, 347.
[6] M. G. Mohamed, W.-C. Chang, S.-W. Kuo, *Macromolecules* **2022**, *55*, 7879.
[7] M. M. Samy, M. G. Mohamed, S.-W. Kuo, *Eur. Polym. J.* **2020**, *138*, 109954.
[8] K. I. Aly, A. A. Amer, M. H. Mahross, M. R. Belal, A. M. M. Soliman, M. G. Mohamed, *Heliyon* **2023**, *9*, e15976.

[9] C.-Y. Chen, W.-C. Chen, M. G. Mohamed, Z.-Y. Chen, S.-W. Kuo, *Macromol. Rapid Commun.* **2023**, *44*, 2200910.
[10] M. G. Mohamed, C.-J. Li, M. O. A. R. Khan, C.-C. Liaw, K. Zhang, S.-W. Kuo, *Macromolecules* **2022**, *55*, 3106.
[11] M. M. Samy, M. G. Mohamed, T. H. Mansoure, T. S. Meng, M. O. A. R. Khan, C.-C. Liaw, S.-W. Kuo, *J. Taiwan Inst. Chem. Eng.* **2022**, *132*, 104110.
[12] R. Yang, L. Xie, N. Li, P. Froimowicz, K. Zhang, *Polym. Chem.* **2022**, *13*, 3639.
[13] S. Mukherjee, N. Amarnath, M. Ramkumar, B. Lochab, *Macromol. Chem. Phys.* **2022**, *223*, 2100458.
[14] S. Appasamy, H. Arumugam, B. Krishnasamy, A. Muthukaruppan, *Macromol. Chem. Phys.* **2023**, *224*, 2200407.
[15] Z. Deliballi, B. Kiskan, Y. Yagci, *Macromolecules* **2020**, *53*, 2354.
[16] M. G. Mohamed, S. W. Kuo, *Macromol. Chem. Phys.* **2019**, *220*, 1800306.
[17] M. M. Samy, M. G. Mohamed, S.-W. Kuo, *Compos. Sci. Technol.* **2020**, *199*, 108360.
[18] S. Huo, P. Song, B. Yu, S. Ran, V. S. Chevali, L. Liu, Z. Fang, H. Wang, *Prog. Polym. Sci.* **2021**, *114*, 101366.
[19] W.-C. Su, F.-C. Tsai, C.-F. Huang, L. Dai, S.-W. Kuo, *Polymers* **2019**, *11*, 201.
[20] F.-L. Jin, X. Li, S.-J. Park, *J Ind Eng Chem* **2015**, *29*, 1.
[21] Z.-M. Zhu, L.-X. Wang, X.-B. Lin, L.-P. Dong, *Polym. Degrad. Stab.* **2019**, *169*, 108981.
[22] C.-F. Huang, W.-H. Chen, J. Aimi, Y.-S. Huang, S. Venkatesan, Y.-W. Chiang, S.-H. Huang, S.-W. Kuo, T. Chen, *Polym. Chem.* **2018**, *9*, 5644.
[23] S. W. Kuo, W. C. Liu, *J. Appl. Polym. Sci.* **2010**, *117*, 3121.
[24] A.-L. Brocas, C. Mantzaridis, D. Tunc, S. Carlotti, *Prog. Polym. Sci.* **2013**, *38*, 845.
[25] T. Vidil, F. Tournilhac, S. Musso, A. Robisson, L. Leibler, *Prog. Polym. Sci.* **2016**, *62*, 126.
[26] R. Gong, Q. Xu, Y. Chu, X. Gu, J. Ma, R. Li, *RSC Adv.* **2015**, *5*, 68003.
[27] J. A. Carioscia, J. W. Stansbury, C. N. Bowman, *Polymer* **2007**, *48*, 1526.
[28] T. Kavalli, R. Wolf, S. Ozen, J. Lalevée, *Eur. Polym. J.* **2022**, *166*, 111031.
[29] J. Ye, Z. Fan, S. Zhang, X. Liu, *J. Appl. Polym. Sci.* **2023**, *140*, e53956.
[30] W.-C. Chen, Z.-Y. Chen, Y. Ba, B. Wang, G. Chen, X. Fang, S.-W. Kuo, *Polymers* **2022**, *14*, 2380.
[31] L. Zhao, X. Xu, W. Xiao, H. Li, H. Feng, C. Liu, Y. Qiao, X. Bai, D. Wang, C. Qu, *Polymers* **2023**, *15*, 1436.
[32] W. Wang, Z. Cao, Z. Wang, *Polym. Adv. Technol.* **2023**, *34*, 1540.
[33] Y.-C. Kao, W.-C. Chen, A. F. M. El-Mahdy, M.-Y.u Hsu, C.-H. Lin, S.-W. Kuo, *Molecules* **2022**, *27*, 5938.
[34] M. Jiang, Y. Liu, C. Cheng, J. Zhou, B. Liu, M. Yu, H. Zhang, *Polym. Test. 96, Int. Conf. Test. Polym., 2nd* **2018**, *69*, 302.
[35] J. D. Jovanovic, M. N. Govedarica, P. R. Dvornic, I. G. Popovic, *Polym. Degrad. Stab.* **1998**, *61*, 87.
[36] S. Sobhani, A. Jannesari, S. Bastani, *J. Appl. Polym. Sci.* **2012**, *123*, 162.
[37] K. Zhang, X. Yu, S.-W. Kuo, *Polym. Chem.* **2019**, *10*, 2387.
[38] P.-H. Sung, C.-Y. Lin, *Eur. Polym. J.* **1997**, *33*, 903.
[39] W.-C. Shih, C.-C. M. Ma, *J. Appl. Polym. Sci.* **1998**, *69*, 51.
[40] Y.-T. Liao, Y.-C. Lin, S.-W. Kuo, *Macromolecules* **2017**, *50*, 5739.
[41] T. Kasemura, S. Takahashi, K. Nishihara, C. Komatu, *Polymer* **1993**, *34*, 3416.
[42] P. Wang, M. Liu, Q. Ran, *Polym. Degrad. Stab.* **2020**, *179*, 109279.
[43] M. G. Mohamed, S.-W. Kuo, *Soft Matter* **2022**, *18*, 5535.
[44] S. W. Kuo, *J. Polym. Res.* **2022**, *29*, 69.
[45] B. Krishnasamy, H. Arumugam, A. Muthukaruppan, *Polym. Polym. Compos.* **2021**, *29*, S1475.
[46] A. S. Mousa, M. G. Mohamed, C. H. Chuang, S. W. Kuo, *Polymers* **2023**, *15*, 1891.
[47] M. G. Mohamed, S. U. Sharma, N.-Y. Liu, T. H. Mansoure, M. M. Samy, S. V. Chaganti, Y.-L. Chang, J.-T. Lee, S.-W. Kuo, *Inter. J. Mol. Sci.* **2022**, *23*, 3174.